ELSEVIER

Plant Science 163 (2002) 33–42

PLANT SCIENCE

www.elsevier.com/locate/plantsci

Overexpression of the cell plate-associated dynamin-like GTPase, phragmoplastin, results in the accumulation of callose at the cell plate and arrest of plant growth

C. Jane Geisler-Lee [a,c], Zonglie Hong [b,c], Desh Pal S. Verma [a,b,c,*]

[a] *Department of Plant Biology, The Ohio State University, Columbus, OH 43210-1002, USA*
[b] *Department of Molecular Genetics, The Ohio State University, Columbus, OH 43210-1002, USA*
[c] *Plant Biotechnology Center, The Ohio State University, 1060 Carmack Road, Columbus, OH 43210-1002, USA*

Received 28 December 2001; received in revised form 4 March 2002; accepted 4 March 2002

Abstract

Phragmoplastin, a dynamin-like GTPase, is associated with cell plate formation in plants. We expressed a phragmoplastin-GFP construct (Phr^G) under the control of a 35S promoter in transgenic tobacco plants. High levels of expression of this chimeric protein in transgenic plants were confirmed by Western blot analysis. T1 seedlings formed morphologically normal cotyledons, but most were unable to develop beyond the first pair of true leaves. Only 5–10% of the seedlings could develop into small plants whose progenies continued to exhibit severe growth defects. The primary root growth was arrested after 7 days and no lateral roots were formed. The mature primary root meristem consisted of disorganized isodiametrically enlarged cells and no recognizable quiescent center or collumela. Adventitious root primordia were initiated in the hypocotyl, but completely arrested at an early stage and contained differentiated treachery elements. The orientation of cell plates was abnormal, suggesting a possible defect in its positioning. However, unlike other cytokinesis mutants, no binucleate or polyploid cells were found. Fluorescence image cytometry studies indicated that Phr^G root meristem cells had 2C levels of DNA and appear to be arrested in G1 stage of the cell cycle. Heavy callose deposition was observed at the nascent cell plate and callose accumulation persisted in new cell walls. Electron microscopy revealed unusual electron dense substances in the maturing cell plate and accumulation of multivesicular bodies around the cell plate. Since phragmoplastin interacts with callose synthase complex, its overexpression may affect accumulation of callose arresting plant growth due to perturbation in cell division progression. © 2002 Published by Elsevier Science Ireland Ltd.

Keywords: Cell plate; Cytokinesis; Phragmoplastin; Vesicle fusion; Callose; Root meristem

1. Introduction

The process of cell plate formation is initiated by fusion of Golgi-derived vesicles to create a de novo structure in the center of phragmoplast [1]. Cytokinesis is completed when the growing cell plate reaches and fuses with the parental cell wall [2–4]. Phragmoplastin is a dynamin-like GTPase, which has been localized at the phragmoplast [5] and has been shown to interact with a subunit of callose synthase complex in yeast 2-hybrid studies [6]. Callose is found in all growing cell plates; however, in young cell walls it disappears, except at plasmodesmata [7]. Callose is not found in Golgi vesicles and is synthesized soon after vesicle fusion at the forming cell plate [1,2]. As the cell plate matures into a cell wall, callose is replaced by cellulose [2]. Changes in cell wall carbohydrate composition may have an impact on cell division and cell fate [8]. Unique carbohydrates in the cell wall have tissue and cell specific distribution and may be involved as positional cues for development or cell fate [9].

The role of cell division in development has not been fully resolved and it has been suggested that division in itself does not regulate development [10]. It is possible that some plant cell cycle genes may play a role in

Abbreviations: MI, mitotic index; Phr^G, transgenic tobacco line expressing wild-type phragmoplastin-GFP; RM, root meristem; SAM, shoot apical meristem; VTV, vesicle-tubule-vesicle.

* Corresponding author. Tel.: +1-614-292-3625; fax: +1-614-292-5379

E-mail address: verma.1@osu.edu (D.P.S. Verma).

0168-9452/02/$ - see front matter © 2002 Published by Elsevier Science Ireland Ltd.
PII: S0168-9452(02)00046-8

development [11,12]. For example, when a dominant negative form of the cell cycle gene for cdc2a kinase was overexpressed in *Arabidopsis*, there was a loss of organization and arrest of embryos [13]. However, when cdc2a kinase was similarly disrupted in tobacco, meristems arrested post-embryonically, but differentiated into morphologically normal tissues [14]. The *Arabidopsis root meristemless* mutant, affecting a glutathione biosynthesis gene, causes loss of cell division in root meristems and leads to the differentiation of meristematic cells into normal tissues [15]. A similar tobacco mutant, *rootless*, also causes cessation of division in postembryonic roots and does not affect cell files or architecture of the root tip [16]. Other cell cycle genes have an effect on organ morphology. For instance, an inhibitor of cyclin dependant kinase (ICK) leads to changes in leaf shape and anatomy when overexpressed in *Arabidopsis* [17]. Mutations in developmental genes, such as *hobbit*, disrupt the root quiescent center leading to a loss of cell division [18,19]. Other mutations, such as *wuschel* and *zwille*, affect the central zone of the shoot apical meristem and result in the reduction of cell division [19,20]. The *shoot meristemless* prevents the formation of the shoot apical meristem (SAM) and causes enlargement and fusion of embryonic shoot [21]. Thus, cell division appears to be neither upstream nor downstream of developmental patterning, but is an integral part of it.

Recently, an increasing number of cytokinesis-defective plant mutants have been described [4,22] (for review see Ref. [1]). Most of the cytokinesis mutations have been found to be lethal and associated with the formation of an abnormal cell plate [23–28]. Some cytokinesis mutants with apparently normal cell plate have also been reported [29]. Mutants, such as *keulle*, *knolle*, and *cytokinesis defective*, result in the partial or complete lack of the cell plate, creating binucleate or polyploid cells [29,30]. The Knolle protein is a cytokinesis-specific syntaxin that facilitates the homotypic fusion of vesicles at the forming cell plate and *knolle* mutants show impaired vesicle fusion [28]. The maize *tan1* and *Arabidopsis ton/fass* mutations cause misorientation of the plane of cell division, but nevertheless develop leaves of normal shape [31–33].

We have shown that phragmoplastin forms helical structures which may wrap around the vesicles to form tubules [34], similar to those formed by dynamin in the presence of GTP-γ-S [35]. Strikingly, many dumbbell-shaped vesicle-tubule-vesicle (VTV) structures have been observed on the forming cell plate [2]. A possible common thread between dynamin and phragmoplastin appears to be that they both form tubular structures in a process possibly controlled by the regulation of their GTPase activity [34–36]. A PCR based screen for T-DNA mutants found an insertion that knocked out expression of one of the *Arabidopsis* homologs of phragmoplastin, ADL1A [37]. This mutant had growth arrested at the early seedling stage, with stunted roots and unexpanded leaf primordia. However, no obvious defects were observed in cytokinesis or in the anatomy of the shoot apical meristem.

To further elucidate the role of phragmoplastin in cell plate formation, we generated transgenic tobacco plants overexpressing phragmoplastin. Transgenic plants exhibited a decrease in mitotic index (MI), formed oblique cell plates and accumulated callose at the forming cell plate. In addition, multivesicular bodies were observed in the vicinity of the forming cell plate.

2. Materials and methods

2.1. Plant materials and growth conditions

Tobacco (*Nicotiana tabacum* cv. Xanthi) seeds were sterilized in 70% ethanol for 5 min followed by treatment with 50% Clorox bleach/0.1% Tween-20 for 10 min. Seeds of transgenic plants were germinated on MS medium (4.3 g/l MS salts, 5 g/l sucrose and 9 g/l agar containing 100 mg/l kanamycin) in a controlled environment chamber at 23 ± 1 °C under constant light. For seed propagation, seedlings were transferred to Metro Mix and grown in a greenhouse at 25 ± 2 °C. The plants were fertilized with 20 mM NH_4NO_3 in half-strength Hoagland's nutrient solution once a week.

2.2. Plant transformation

Transgenic tobacco plants were obtained through *Agrobacterium*-mediated leaf disc transformation using the plasmid pBI121-EGP [5], expressing the coding sequence for soybean phragmoplastin fused with GFP (Phr^G). Control plants were transformed with pBI-GFP that expresses the GFP protein under the control of the CaMV 35S promoter. Plants were also transformed with CaMV 35S::phragmoplastin without the GFP fusion. They did not appear different to those with the GFP fused phragmoplastin (Phr^G) and hence the latter was used in these experiments to facilitate observations.

2.3. Protein extraction and Western blot analysis

Sterile seeds were germinated on MS medium containing 100 mg/l kanamycin. Ten-day-old seedlings were homogenized in liquid nitrogen and resuspended in SDS-loading buffer. Western blot analysis was performed as described previously, using antibodies against soybean phragmoplastin [5,38].

2.4. Measurements of root growth

For root growth measurements, T1 seeds of control and Phr^G plants were sown and aligned individually on Petri dishes containing MS medium. The plates were placed vertically and maintained in a tissue culture room at 26 °C. The length of the primary roots from the base of the hypocotyl to the root tip was measured and recorded weekly for 4 weeks after germination.

2.5. Mitotic index and nuclear DNA contents

Root tips (2 mm long) of tobacco seedlings were fixed in FAA solution (5% formalin: 5% acetic acid: 50% ethanol) mixed with phosphate buffered saline (50/50) for 2 h followed by a rinse in 1:1 ratio of 95% alcohol and 37.5% HCl for 2 min. The root tips were stained with 1 μg/ml of 4′-6′-diamin-dino-2-phenylindole (DAPI; Sigma Chemical Co.) in PBS for 20 min. The cells were viewed under an Axiophot Zeiss microscope with appropriate filters for DAPI. The mitotic index was calculated as the percentage of cells with condensed chromatin or cells at mitosis. Longitudinal sections of root tips (2 mm long) were made with a razor blade under a dissecting microscope. The fluorescence intensity of nuclei in the columella, meristematic areas and elongating region were measured using Scion Image software package β3b [39]. The DNA contents of the control plant guard cells were used as internal standard (2C; [40]). For this purpose, epidermal cell layer from a leaf was peeled and treated in the same manner as above.

2.6. Light microscopy

Root tips of 4-week-old plants were fixed in FAA solution for 4 h, dehydrated in alcohol series and infiltrated with paraffin (Paraplast). Sections (8 μm) were stained with 1% Safranin O in 50% alcohol and 1% Fast Green in 95% alcohol. The sections were viewed and photographed under an Axiophot Zeiss microscope (Carl Zeiss, Inc.).

2.7. Histochemical staining for callose

Root tips were fixed in FAA solution for 2 h and rinsed with a 1:1 solution of 95% ethanol: 37.5% HCl for 2 min. The tissue was washed thoroughly with PBS and the samples were stained with Aniline blue (1 μg/ml) in PBS for 20 min to detect callose [41], followed by staining with ethidium bromide (1 μg/ml) for 2 min to detect nuclei. The root tips were squeezed between a glass slide and a cover slip to release cells. The cells were viewed using a fluorescent microscope with appropriate filters and images were recorded digitally. The percentage of the cell walls with callose was measured as the total number of new cell walls stained with Aniline blue divided by the total number of the root tip cells counted. These are the minimum estimates since the concentration of callose at the cell plate was not taken into consideration.

2.8. Electron microscopy

Root and shoot tips (2–3 mm long) of 4- to 10-day-old seedlings were fixed in 2% glutaraldehyde in 75 mM phosphate buffer, pH 7.2 and were post fixed in 2% osmium in the same buffer. An acetone dehydration series was performed and the samples were embedded in Spurr resin. Ultrathin sections were stained with uranyl acetate followed by lead citrate. Micrographs were taken using a Phillips CM12 transmission electron microscope (Philips Electronic Instruments Co., Mahwah, NJ) at 60 kV.

3. Results

3.1. Overexpression of phragmoplastin arrests growth of transgenic plants

Our previous results demonstrated that a chimeric phragmoplastin-GFP (Phr^G) protein is targeted to the forming cell plate when expressed in cultured tobacco BY-2 cells [5]. Cells expressing Phr^G were elongated, divided slowly compared to the control cells expressing GFP only, and often had altered cell division orientation. To study how these changes may affect the architecture of a plant, we expressed Phr^G in tobacco plants and examined 25 independent transgenic lines in detail. Twenty lines displayed variable phenotypes, including chlorotic leaves and arrested growth of the primary root, shoot and adventitious roots (Fig. 1B). The leaves of all transgenic lines appeared etiolated and had an expanded central vein with greatly reduced blade area. The primary roots were stunted and no lateral roots emerged in the majority (90%) of seedlings. These phenotypes were the same as those from plants overexpressing phragmoplastin alone (see Section 2). Control plants expressing GFP alone did not display any visible phenotype (Fig. 1A).

Progeny from transgenic Phr^G line No. 2 exhibited a 3:1 segregation ratio for kanamycin-resistance, suggesting that there was only one T-DNA insertion in this transgenic line. Southern blot analysis of genomic DNA confirmed that the transgene was inserted in a single locus (data not shown). This line was used in rest of the experiments. In the T1 population of Phr^G line No. 2, 90% of the seedlings were unable to grow beyond the stage of first or second pair of true leaves and died as a consequence. About 10% of the plants survived and were able to set seeds, although the plant size and seed

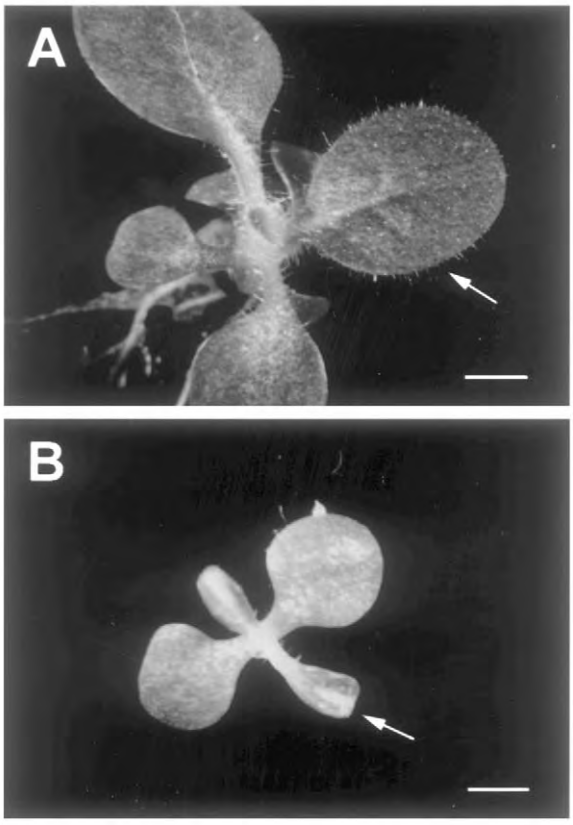

Fig. 1. Phenotypes of tobacco transgenic plants overexpressing phragmoplastin (Phr^G). (A) Control seedlings transformed with GFP alone. (B) Transgenic seedlings expressing Phr^G. Note that whereas cotyledons were apparently normal, the first pair of true leaves (arrows) in transgenic plants remained small and the central vein or entire leaf area was chlorotic. Most of the mutant plants did not develop beyond the first pair of true leaves.

numbers were very much reduced compared to the control plants. Progeny from the surviving plants continued to exhibit severe (90%) and mild (10%) mutant phenotypes. The latter type expressed very low levels of the transgene (data not shown), which may be due to cosuppression of the endogenous phragmoplastin gene in these lines. The reason for the continued variability is, however, not clear.

Western blot analysis using the purified antibody to soybean phragmoplastin showed a unique protein band in transgenic plants (94 kDa: Fig. 2B, lane 2) that corresponded to the size of the chimeric protein of GFP (26 kDa) plus phragmoplastin (68 kDa), confirming that the chimeric protein is expressed in Phr^G plants. An additional band (68 kDa) corresponding to the tobacco native phragmoplastin was also visible in both control and transgenic plants, resulting from a cross-reaction [38]. These data also suggest that the expression of the native phragmoplastin was not affected in Phr^G lines due to the insertion of the chimeric phragmoplastin gene.

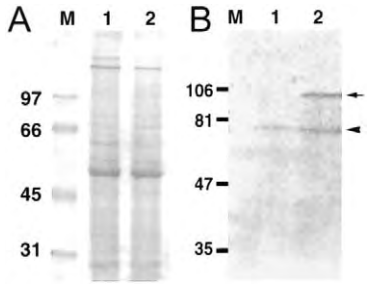

Fig. 2. SDS-PAGE and Western blot analysis of protein extract from leaves of the control and Phr^G seedlings. (A) Total proteins were extracted from 10-day-old seedlings and resolved on SDS-PAGE followed by staining with Coomassie blue. M, molecular weight markers in kDa; Lane 1, control seedlings transformed with pBI-GFP; Lane 2, Phr^G transgenic seedlings. (B) Western blot of the same samples as in (A) except that the molecular markers were replaced by prestained protein markers. Purified rabbit IgG against *E. coli*-expressed soybean phragmoplastin [38] was used as primary antibody and horseradish peroxidase-conjugated goat IgG against rabbit IgG was used as the second antibody and detected by the ECL Western blot system (Amersham). 94 kDa (arrow), GFP-phragmoplastin protein; 68 kDa (arrowhead), native phragmoplastin.

3.2. *Overexpression of Phr^G affects orientation of the cell plate*

We analyzed the pattern of cell plate formation during early female gametophyte development in transgenic plants that were able to grow until flowering. Longitudinal sections of ovules at early stages of megaspore development showed that at the 4-cell stage, the orientation of the cell wall was altered compared to that of control plants (Fig. 3). The orientation of cell plates was altered between megaspores one and two and between megaspores three and four (Fig. 3B), suggesting that cell plate formation in both mitosis and meiosis is affected in the transgenic lines. While the cell plate was completed in both types of megaspores, the divisions

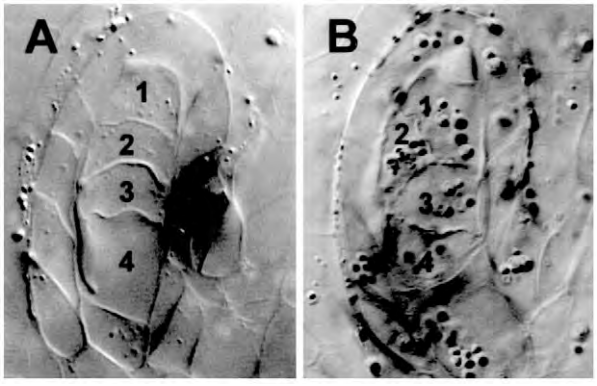

Fig. 3. Effect of overexpression of phragmoplastin on the orientation of the cell plate in female gametophyte of tobacco. Longitudinal sections through ovule: (A) control; (B) Phr^G plants. Note the transverse cell walls in both mitotic and meiotic cell divisions in (A), while oblique cell walls in the Phr^G megagametophytes. The numbers 1–4 represent products of successive meiotic and mitotic cell divisions of megagametophyte initial. Cell No. 1 represents the megaspore cell.

were not transverse as observed in the control female gametophyte (Fig. 3A). It is possible that this misorientation may affect megaspore development, which is indicated by the very small number of seeds produced by Phr^G plants.

3.3. Decrease in mitotic index and arrest of root growth in Phr^G seedlings

Measurements of the root length indicated that the radicles (embryonic root) of both the control and Phr^G seeds emerged from the seed coat at the same time (at about day 3 after seed imbibition). The root began to grow in the control seeds immediately, but growth of the Phr^G roots was severely retarded. This limited growth was primarily due to cell expansion since the mitotic activity was very low in this tissue (see below). This was apparent because of the difference in the sizes of cells in the control and Phr^G roots. The primary roots of the control plants showed rapid growth during the first week and steady growth for another 3 weeks of observation, with secondary roots appearing around 9–10 days (Fig. 4(A), filled circles). In Phr^G seedlings, growth was severely retarded after 1 week and no secondary roots were formed (Fig. 4(A), open circles).

To determine the rate of cell division in root tips of the Phr^G plants, the mitotic index (MI) was measured. As shown in Fig. 4(B), the MI of the Phr^G roots was much lower than that of the control plants and dropped steadily to zero within 2 weeks after germination. The MI of the control plants was $\approx 1.5\%$ at day 13, which was higher than that at day 7 in the Phr^G plants. Aniline blue staining showed that the percentage of the cell walls with callose in Phr^G cells steadily increased to 15% by day 13 (Fig. 4C) when the MI dropped to zero (Fig. 4B). However, very little callose was found in the control cell walls during the second week.

3.4. Loss of the quiescent center and arrest of the cells at the G1 phase in Phr^G roots

Root architecture in Phr^G seedlings showed a disorganized cell mass that lacked distinct cell files. No quiescent center or columella could be recognized anatomically compared to control at the same age (Fig. 5). The enlarged and vacuolated cells in the Phr^G root meristem may indicate the loss of undifferentiated state of the meristematic initials. In addition, irregular cubic shape of the cells indicated that they had undergone isodiametric expansion. This is in contrast to root meristems which have stopped dividing due to the disruption of cell cycle [14], or in the *hobbit*, *rml*, or *rootless* mutants, where there is no disruption of the cell files and expansion remains axialized [15,16]. This indicates that Phr^G overexpression did not simply shut down cell division, but allowed some divisions which

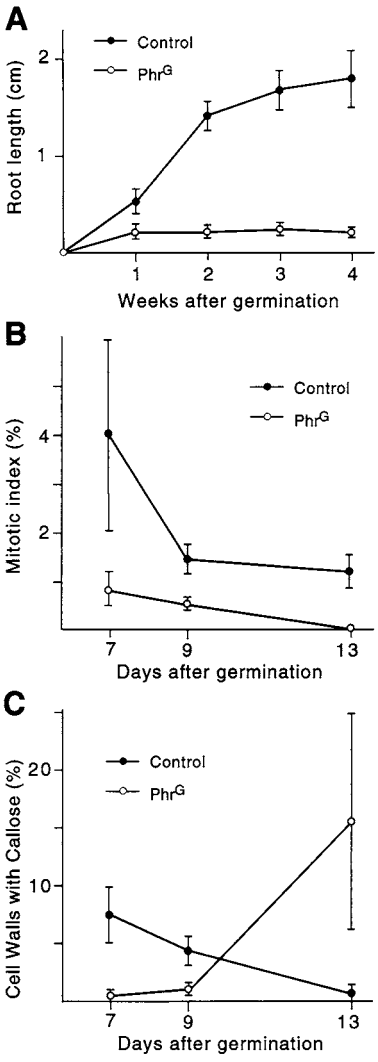

Fig. 4. Rate of cell division and the growth of roots in control and Phr^G transgenic plants. (A) Root growth during the first 4 weeks after germination. (B) Mitotic indices of root tip cells stained with DAPI. (C) Callose accumulation at the cell plate and new cell walls. Root tissue was stained with Aniline blue and the fluorescent labeled new cell walls were recorded at different time intervals (see Fig. 7).

disrupted cell files and the architecture of the RAM prior to cessation of all divisions.

To determine the phase of the cell cycle in which the root meristem cells were arrested, we measured DNA contents of the root cells including columella, meristematic area and elongating region. The relative DNA contents in these regions was compared to nuclei of wild-type leaf guard cells which are presumed to be 2C as in *Arabidopsis* [40]. No cells containing 4C DNA were detected in the root tip region of 3-week-old Phr^G seedlings (Fig. 5D), whereas a significant number of control root tip cells contained 4C DNA (two sets of 2C nuclear DNA in the S phase; Fig. 5C). This suggests that the Phr^G root cells may be arrested at the G1 phase of the cell cycle. However, this phenotype is indirect, as phragmoplastin is unlikely to affect cell cycle progres-

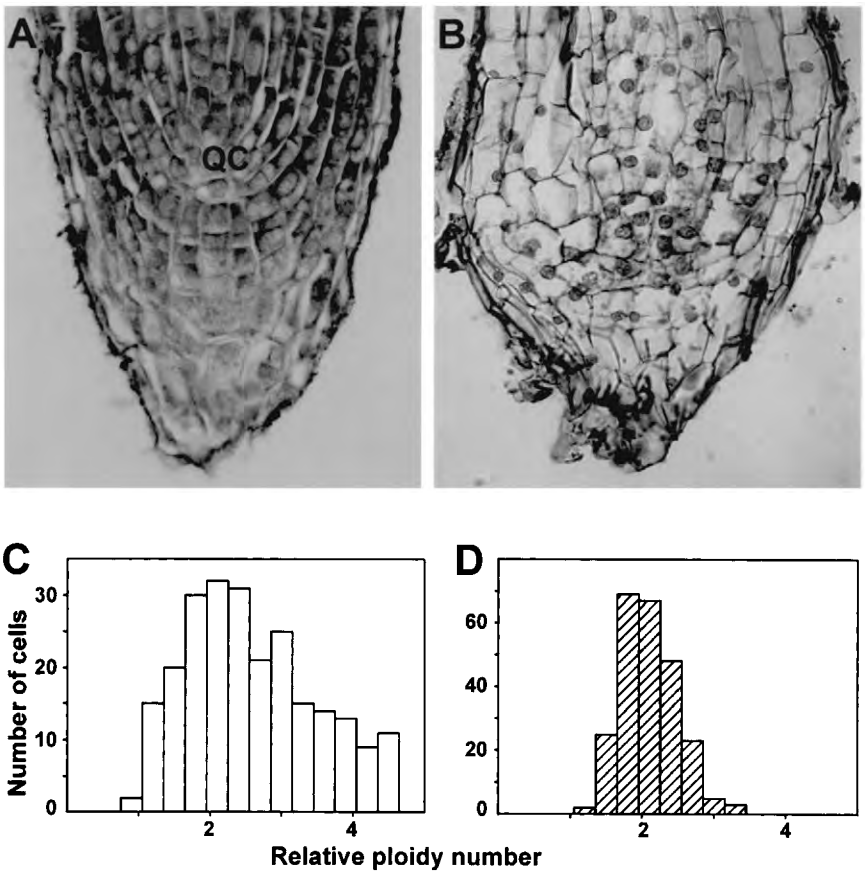

Fig. 5. Root meristems of control and Phr^G transgenic seedlings. (A, B) Longitudinal sections of root tips of 4-week-old control and Phr^G seedlings. Root tips were fixed and embedded in paraffin, stained with Safranin O and Fast Green. Note the loss of quiescent center and columella cells in Phr^G roots. (C, D) Relative ploidy levels of root tip cells. QC, quiescent center.

sion, based on its proposed role in building cell plate [1]. This may be due to a delay in symplastic signals that normally affects cell growth [8]. No multinucleate or polyploid cells were found in Phr^G seedlings, indicating that cell plates in Phr^G roots were completed and had not degenerated as in several cytokinesis mutants.

3.5. *Arrest of adventitious root primordia in Phr^G root*

Secondary roots in control plants began to develop during the second week of germination. The Phr^G plants did not form any secondary roots but rather initiated several adventitious root primordia along the lower hypocotyl region after 3–4 weeks (Fig. 6A). These adventitious root primordia arrested at a very early stage and were unable to develop further into lateral roots. Cells in these primordia differentiated into vessels and tracheid-like structures (Fig. 6B). Unlike the primary root, the cells of the entire lateral root meristem had differentiated into a very unusual cell type. This indicates that, in addition to loss of division and differentiation, there was an alteration of cell fate in cells expressing Phr^G.

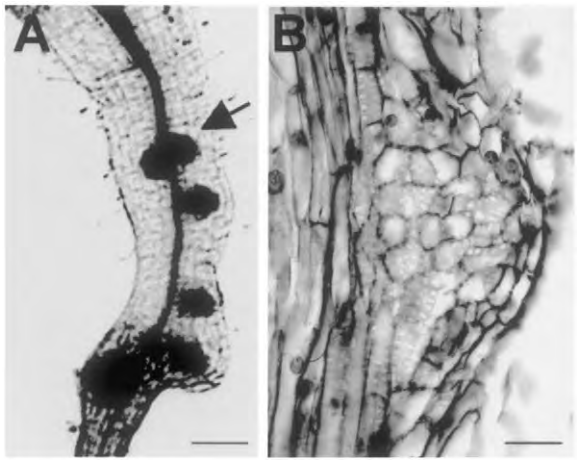

Fig. 6. Adventitious root primordia in the hypocotyl region of Phr^G seedlings. (A) Four-week-old tobacco seedlings were fixed and stained with Safranin O and Fast Green. Multiple adventitious root primordia (arrow) emerged on the lower hypocotyl of the Phr^G seedling. (B) Enlarged view of a longitudinal section of an adventitious root primordium. Note the tracheid and vessel-like structures in the primordium that has not yet emerged from the cortex.

3.6. Increased deposition of callose at the cell plate and its persistence in new cell walls in the Phr^G seedlings

We have recently observed that phragmoplastin interacts with callose synthase at the forming cell plate [42]. To determine if the overexpression of phragmoplastin had any effect on callose deposition at the nascent cell plate, we localized callose by fluorescence microscopy using Aniline blue staining [41]. The cell plate of the control plants was stained as a thin line with few punctuated structures (Fig. 7C, arrow). In root tips of 1-week-old Phr^G seedlings (in which low cell division activity existed; Fig. 4B), the intensity of callose staining in the nascent cell plates was much higher than that in the control plants. Cell plates were stained as a very bright and thick lens-shaped structure (Fig. 7D, arrow). About 15% of the cells in the 2-week-old root tips of Phr^G seedlings, including columella, meristematic and elongating regions, had a part of the cell wall stained with Aniline blue (see Fig. 4C). Although the MI in the root of Phr^G cells was very low at this time, callose appeared to persist in mature cell plates of these cells. The accumulation of callose in Phr^G cells may be due to a higher rate of callose synthesis and/or a delay in its degradation that occurs normally during cell plate maturation [1].

3.7. Formation of large vesicles on the cell plate and accumulation of multivesicular bodies in cells overexpressing phragmoplastin

We analyzed the ultrastructure of the forming cell plate in the Phr^G cells and compared it with the control cells (Fig. 8). While the structure of the forming cell plate in control cells was similar to that described by Samuels et al. [2], the developing tubular network in Phr^G cells contained more electron dense material (Fig. 8C,D). Numerous large vesicular bodies (arrows in Fig. 8C) were found to be associated with the forming cell plate and many multivesicular bodies appeared (Fig. 8D). These structures are not present in the control cell plate (Fig. 8A). In addition, the angle of cell plate fusing with the parental cell wall is altered making an oblique cell wall as observed in BY2 cells overexpressing phragmoplastin [5].

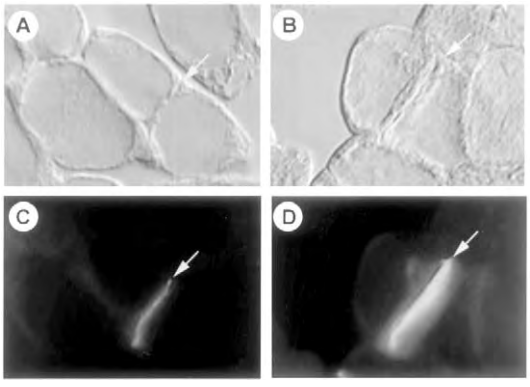

Fig. 7. Aniline-blue staining of callose on the forming cell plates of tobacco root tip cells. Root tips of the control (A) and Phr^G seedlings (B) were fixed and stained with Aniline blue and ethidium bromide. Cells were photographed using a differential interface contrast (DIC) lens. Arrows indicate the position of cell plates. Fluorescent micrographs of the same field were taken using a UV filter (C, D). The cell plate of the control plants (C) was stained as a thin line, whereas that of the Phr^G seedlings (D) was seen as a thick, lens shaped structure.

4. Discussion

4.1. Overexpression of phragmoplastin affects the rate of cell division in both root and shoot meristems

Several cytokinesis mutants, including *cyt1*, *cyd1*, *keule*, *knolle*, *ttn* and *tso1,* form incomplete cell walls, develop partial cell plates or produce multinucleated/polyploid cells [23–27,29–31]. The phenotype of the Phr^G plants was different from those and other cytokinesis mutants described to date [1]. Embryo development in most cytokinesis mutants is affected; an exception is *cyd1*, which displays abnormality in the whole plant from shoot and vegetative meristem to differentiated cells [30]. The process of cytokinesis in Phr^G cells, once started, was able to proceed to completion. However, callose accumulation, which normally disappears as the cell plate matures into a cell wall, persisted much longer in Phr^G cells. This may indicate either an overaccumulation of or failure to remove callose, or a delay in cell plate maturation altogether. This phenomenon resulted in alteration of the direction of cell plate elongation as observed earlier in BY2 cells [5] and was also apparent in megagametophyte cell division (Fig. 3). A perturbation in cell plate growth appears to result in the complete arrest of growth of the root and shoot meristems.

The loss of RAM structure and the arrest of adventitious root primordia in the Phr^G plants are quite different from *rootless* and *root meristemless*, which cause the loss of meristematic activity without disrupting the structure of RAM. It was also different from the *hbt* (*hobbit*) mutant reported to have no recognizable quiescent center and no mitotically active RAM [18]. In a T-DNA knockout mutant of one of the *Arabidopsis* phragmoplastin homologs, ADL1A, growth was also arrested without affecting the SAM organization, although RAM structure was not described [37]. These mutants could be rescued by the addition of sucrose, which might indicate growth was arrested due to lack of carbon supply. This is consistent with yellowing of the leaves and suggests that phragmoplastin has other functions in the cells. A chloroplast localized isoform of phragmoplastin has been identified [43]. There are, in

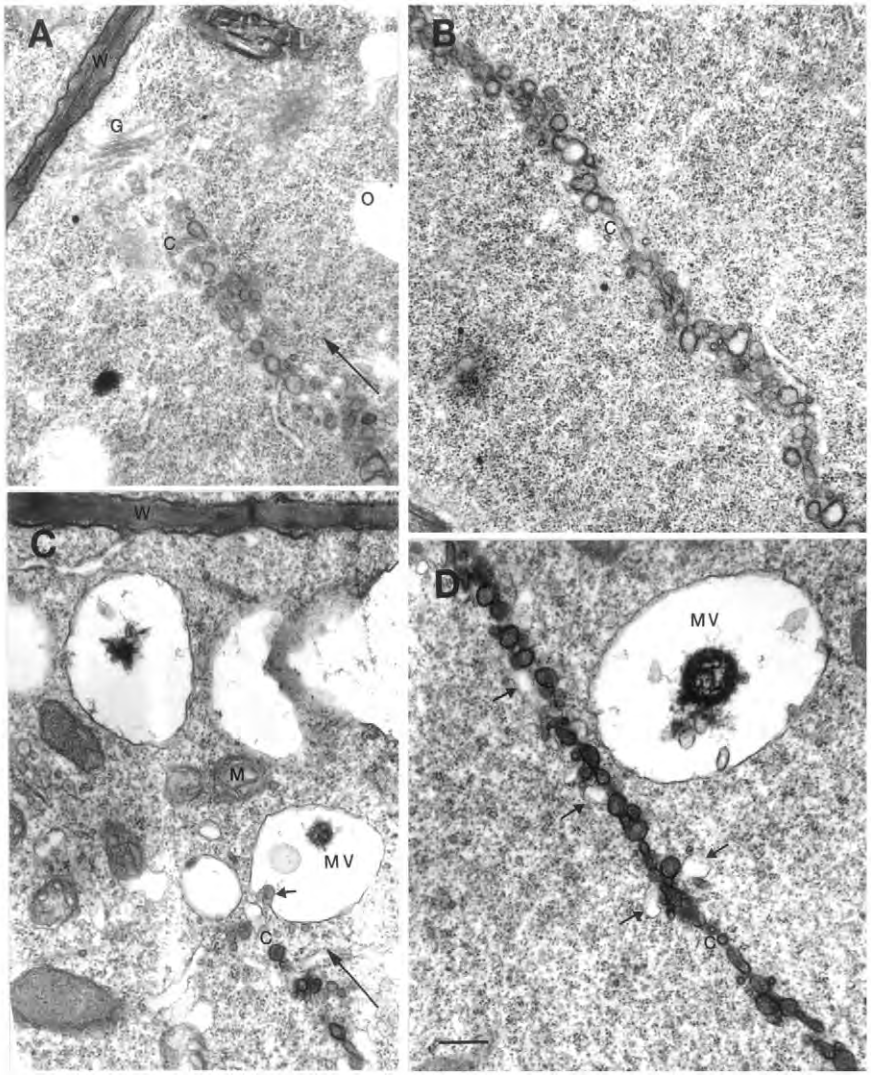

Fig. 8. Electron micrographs of the forming cell plates in control and Phr^G root cells. (A) The T-junction area of the cell plate in a control cell. The direction (arrow) of the growing cell plate (c) was almost perpendicular to the mother cell wall (w). Golgi bodies (G) are present in the T-junction area. Oil bodies (O), but not vacuoles, are found in the path of the growing cell plate. (B) The middle section of the cell plate the same control cell shown in (A). The cell plate is a continuous structure of interconnected tubules. (C) Forming cell plate in Phr^G cell. Multivesicular bodies (MV) filled with electron-dense material are present in this area. Cell plate vesicles (small arrow) are found to fuse with the multivesicular bodies. The large arrow points to the direction of the growing cell plate that is not perpendicular to the parental cell wall and results in the formation of oblique cell plate (see [5]). M, mitochondrion. (D) The middle section of the cell plate in the same Phr^G cell as in (C). Numerous electron-light, large vesicular bodies are found to be associated with the cell plate. These structures are not present in the control cell plate (B). The tubular structures of the forming cell plate are filled with darker contents compared to the control cell plate shown in (B). Multivesicular bodies (MV) filled with dark deposits are seen frequently. Scale bar for A–D, 0.45 μm.

addition, 16 isoforms of this sequence in *Arabidopsis* [1], which suggests a wider role of this group of proteins in plant development.

Since phragmoplastin can form heterodimers [34] and multiple forms of phragmoplastin occurs in a cell, it is likely that other interactions play some role in the complete arrest of growth. It is interesting to note that differentiation proceeded in the lateral root primordia in the absence of new cell generation from the meristem. These data suggest that the initiation of new primordia, their maintenance and differentiation are distinct and independent processes. Furthermore, the reduction in MI and alteration in the pattern of cell plate formation does not affect organ formation, which is consistent with the *tangled* mutant in maize [4,32].

4.2. Persistence of callose in phragmoplastin-overexpressing cells appears to slow down cell plate maturation

The cell plate and young cell walls of the Phr^G seedlings contain more callose than those of the control cells (Fig. 7). The callose persists for 2–3 weeks post germination when there is no mitotic activity in this

tissue (Fig. 4B). A possible mechanism which may account for this over-deposition of callose is an increased activity of callose synthase or a delay in callose degradation, which needs to be replaced by cellulose during cell plate maturation [2]. A *korrigan* mutant affecting 1,4-β-glucanase has been shown to arrest cell plate maturation [44]. Callose synthase is turned on after the initial vesicle fusion stage and reaches maximum levels during the tubular network consolidation phase when cellulose deposition starts [2]. In light of our recent observation that phragmoplastin interacts with a cell plate-specific callose synthase [42], it is possible that overexpression of phragmoplastin may increase callose synthase activity and cause the excessive deposition of callose in the Phr^{G} plants. The persistence of callose may cause a delay in cell plate maturation as is also observed in *hobbit* mutants.

4.3. Possible role of phragmoplastin in creating tubular networks at the forming cell plate

EM studies using the high-pressure cryofixation technique showed that cell plate development can be divided into morphologically distinct steps. These include fusion of Golgi-derived vesicles, development of the tubulo-vesicular network (TVN), generation of the fenestrated sheet and fusion of the cell plate with the parental wall [2,3]. Phragmoplastin appears to be involved in the formation of tubulo-vesicular structures at the cell plate. We have demonstrated that phragmoplastin contains two self-assembly domains, SA1 and SA2 [34]. The intermolecular interaction between SA1 and SA2 leads to the formation of a polymer with a staggered, contoured spiral structure. The helical arrays of the phragmoplastin may wrap around the vesicles in the cell plate region and facilitate the formation of a vesicle-tubule-vesicle structure resembling the dumbbell-shaped structures observed by Samuels et al. [2]. Recently, ADL1 (phragmoplastin) antibodies have been localized around these tubular structures in endosperm cells [45], supporting our model of membrane tubulization mediated by phragmoplastin at the forming cell plate [1].

The process of vesicle-tubule-vesicle formation may require a precise regulation of phragmoplastin GTPase activity. The GTP-bound form of phragmoplastin is required for the formation of phragmoplastin helical arrays and GTP hydrolysis depolymerizes phragmoplastin [34]. The inhibition of this activity is necessary to form long tubules and it may be facilitated by high levels of Ca^{2+} known to be present in the vicinity of the cell plate [46,47]. Ca^{2+} has been found to inhibit dynamin GTPase activity [36] and the inhibition of GTPase results in the formation of tubular structures [35]. The expression of a GTPase-minus mutant of phragmoplastin (Phr^{KM}) results in the persistence of many tubular structures in the forming cell plate (Hong, Geisler-Lee and Verma, unpublished data), similar to what has been shown in the expression of a dynamin GTPase mutant in mammalian cells [48] or in the presence of GTP-γ-S [35,49]. Furthermore, such a mutation in dynamin has been shown to alter vesicle budding from the trans-Golgi, a situation observed in cells overexpressing mutated phragmoplastin (unpublished data). Overexpression of phragmoplastin may affect membrane tubulization process. The elucidation of the exact mechanism of callose deposition at the forming cell plate may be facilitated by detailed analysis of the callose synthase complex that we have recently identified and isolated and found to be interacting with phragmoplastin [6,42].

Acknowledgements

The authors thank Dr Ashton Delauney and Dr Matt Geisler for their help in the preparation of this manuscript. This work was supported by grants (NSF 9724014 and 0095112) from the National Science Foundation, USA.

References

[1] Verma D.P.S., Cytokinesis and building of the cell plate in plants, Ann. Rev. Plant Physiol. Plant Mol. Biol. 52 (2000) 751–784.
[2] Samuels A.L., Giddings T.H., jr, Staehelin L.A., Cytokinesis in tobacco BY-2 and root tip cells, J. Cell Biol. 130 (1995) 1345–1357.
[3] Staehelin L.A., Hepler P.K., Cytokinesis in higher plants, Cell 84 (1996) 821–824.
[4] Smith L.G., Divide and conquer: cytokinesis in plant cells, Curr. Opin. Plant Biol. 2 (1999) 447–453.
[5] Gu X., Verma D.P.S., Dynamics of phragmoplastin in living cells during cell plate formation and uncoupling of cell elongation from the plane of cell division, Plant Cell 9 (1997) 157–169.
[6] Hong Z., Zhang Z., Olson J.M., Verma D.P.S., A novel UDP-glucose transferase forms a complex with callose synthase and interacts with phragmoplastin at the forming cell plate, Plant Cell 13 (2001) 769–780.
[7] Northcote H., Davey R., Lay J., Use of antisera to localize callose, xylan and arabinogalactan in the cell-plate, primary and secondary walls of plant cells, Planta 178 (1989) 353–366.
[8] Strauss E., When walls can talk, plant biologists listen, Science 282 (1998) 28–29.
[9] Freshour G., Clay R.P., Fuller M.S., Albersheim P., Darvill A.G., Hahn M.G., Developmental and tissue-specific structural alterations of the cell-wall polysaccharides of *Arabidopsis thaliana* roots, Plant Physiol. 110 (1996) 1413–1429.
[10] Doonan J., Social controls on cell proliferation in plants, Curr. Opin. Plant Biol. 3 (2000) 482–487.
[11] Traas J., Bellini C., Nacry P., Kronenberger J., Bouchez D., Caboche M., Normal differentiation patterns in plants lacking microtubular preprophase bands, Nature 375 (1995) 676–677.
[12] Meijer M., Murray A.H., Cell cycle controls and the development of plant form, Curr. Opin. Plant Biol. 4 (2001) 44–49.
[13] Hemerly A.S., Ferreira P.C., Van Montagu M., Engler G., Inze D., Cell division events are essential for embryo patterning and

morphogenesis: studies on dominant negative cdc2At mutants of *Arabidopsis*, Plant J. 23 (2000) 123–130.
[14] Hemerly A., de Almeida Engler J., Bergounioux C., Van Montagu M., Engler G., Inze D., Ferreira P., Dominant negative mutants of the Cdc2 kinase uncouple cell division from iterative plant development, EMBO J. 14 (1995) 3925–3936.
[15] Cheng J.C., Seeley K., Sung K., *RML1* and *RML2*, *Arabidopsis* genes required for cell proliferation at the root tip, Plant Physiol. 107 (1995) 365–376.
[16] Pelese F., Megnegneau B., Sotta B., Sossountzov L., Caboche M., Miginiac E., Hormonal characterization of a nonrooting naphthaleneacetic acid tolerant tobacco mutant by an immunoenzymic method, Plant Physiol. 89 (1989) 86–92.
[17] Wang E., Zhou Y., Gilmer Y., Whitwill Y., Fowke L., Expression of the plant cyclin-dependent kinase inhibitor ICK1 affects cell division, plant growth and morphology, Plant J. 24 (2000) 613–623.
[18] Willemsen V., Wolkenfelt V., de Vrieze G., Weisbeek P., Scheres B., The *HOBBIT* gene is required for formation of the root meristem in the *Arabidopsis* embryo, Development 125 (1998) 521–531.
[19] Mayer K.F.X., Schoof H., Haecker A., Lenhard M., Jurgens G., Laux T., Role of *WUSCHEL* in regulating stem cell fate in the *Arabidopsis* shoot meristem, Cell 95 (1998) 805–815.
[20] Moussian B., Schoof H., Haecker A., Jurgens G., Laux T., Role of the *Zwille* gene in the regulation of central shoot meristem cell fate during *Arabidopsis* embryogenesis, EMBO J. 17 (1998) 1799–1809.
[21] Endrizzi K., Moussian B., Haecker A., Levin J., Laux T., The *SHOOT MERISTEMLESS* gene is required for maintenance of undifferentiated cells in *Arabidopsis* shoot and floral meristems and acts at a different regulatory level than the meristem genes *WUSCHEL* and *ZWILLE*, Plant J. 10 (1996) 967–979.
[22] Heese M., Mayer U., Jurgens G., Cytokinesis in flowering plants: cellular processes and developmental integration, Curr. Opin. Plant Biol. 1 (1998) 486–491.
[23] Nickle T.C., Meinke D.W., A cytokinesis-defective mutant of *Arabidopsis* (*cyt1*) characterized by embryonic lethality, incomplete cell walls, and excessive callose accumulation, Plant J. 15 (1998) 321–332.
[24] Liu C., Sue J., Wang T.L., cyd, a mutant of pea that alters embryo morphology, is defective in cytokinesis, Development 16 (1995) 321–331.
[25] Assaad F.F., Mayer U., Wanner G., Jurgens G., The *KEULE* gene is involved in cytokinesis in *Arabidopsis*, Mol. Gen. Genet. 253 (1996) 267–277.
[26] Liu C.M., Meinke C.M., The titan mutant of *Arabidopsis* are disrupted in mitosis and cell cycle control during seed development, Plant J. 16 (1998) 21–31.
[27] Lukowitz W., Mayer W., Jurgens G., Cytokinesis in the *Arabidopsis* embryo involves the syntaxin-related *KNOLLE* gene product, Cell 84 (1996) 61–71.
[28] Lauber M.H., Waizenegger I., Steinmann T., Schwarz H., Mayer U., Hwang U., Lukowitz W., Jurgens G., The *Arabidopsis* KNOLLE protein is a cytokinesis-specific syntaxin, J. Cell Biol. 139 (1997) 1485–1493.
[29] Liu Z., Running Z., Meyerowitz E.M., *TSO1* functions in cell division during *Arabidopsis* flower development, Development 124 (1997) 665–672.
[30] Yang M., Nadeau J.A., Zhao L., Sack F.D., Characterization of a cytokinesis defective (*cyd1*) mutant of *Arabidopsis*, J. Exp. Bot. 50 (1999) 1437–1446.
[31] Smith L.G., Hake S., Sylvester A.W., The *tangled 1* mutation alters cell division orientations throughout maize leaf development without altering leaf shape, Development 122 (1996) 481–489.
[32] Trass J., Laufs P., Cell cycle mutants in higher plants: a phenotypical overview, in: Francis D., Dudits D., Inze S. (Eds.), Plant Cell Division, Portland Press Research Monogram, UK, 1998, pp. 319–336.
[33] Torres-Ruiz R.A., Jurgens G., Mutations in the *FASS* gene uncouple pattern formation and morphogenesis in *Arabidopsis* development, Development 120 (1994) 2967–2978.
[34] Zhang Z., Hong Z., Verma D.P.S., Phragmoplastin polymerizes into spiral coiled structures via intermolecular interaction of two self-assembly domains, J. Biol. Chem. 275 (2000) 8779–8784.
[35] Takei K., McPherson P.S., Schmid S.L., DeCamilli P., Tubular membrane invaginations coated by dynamin rings are induced by GTP-γ-S in nerve terminals, Nature 374 (1995) 186–189.
[36] Liu J.P., Powell K.A., Sudhof T.C., Robinson P.J., Dynamin I is a Ca^{2+}-sensitive phospholipid-binding protein with very high affinity for protein kinase C, J. Biol. Chem. 269 (1994) 21043–21050.
[37] Kang B., Busse J.S., Dickey C., Rancour D.M., Bednarek S.Y., The *Arabidopsis* cell plate-associated dynamin-like protein, ADL1Ap, is required for multiple stages of plant growth and development, Plant Physiol. 126 (2001) 47–68.
[38] Gu X., Verma D.P.S., Phragmoplastin, a dynamin-like protein associated with cell plate formation in plants, EMBO J. 15 (1996) 695–704.
[39] Szymanski D.B., Marks M.D., *GLABROUS1* overexpression and *TRIPTYCHON* alter the cell cycle and trichome cell fate in *Arabidopsis*, Plant Cell 10 (1998) 2047–2062.
[40] Melangro J.E., Mehrotra B., Coleman A.W., Relationship between endopolyploidy and cell size in epidermal tissue of *Arabidopsis*, Plant Cell 5 (1993) 1661–1668.
[41] Smith M.M., McCully M.E., Enhancing aniline blue fluorescent staining of cell wall structures, Stain Technol. 53 (1978) 79–85.
[42] Hong Z., Delauney A.J., Verma D.P.S., A cell-plate specific callose synthase and its interaction with phragmoplastin and UDP-glucosyltransferase, Plant Cell 13 (2001) 755–768.
[43] Kang S.G., Jin J.B., Piao H.L., Pih K.T., Jang H.J., Lim J.H., Hwang I., Molecular cloning of an *Arabidopsis* cDNA encoding a dynamin-like protein that is localized to plastids, Plant Mol. Biol. 38 (1998) 437–447.
[44] Zuo J., Niu Q.W., Nishizawa N., Wu Y., Kost B., Chua N.H., *KORRIGAN*, an *Arabidopsis* endo-1,4-β-glucanase, localizes to the cell plate by polarized targeting and is essential for cytokinesis, Plant Cell 12 (2000) 1137–1152.
[45] Otegui M.S., Mastronarde D.N., Kang B.H., Bednarek S.Y., Staehelin L.A., Three-dimensional analysis of syncytial-type cell plates during endosperm cellularization visualized by high resolution electron tomography, Plant Cell 13 (2001) 2033–2051.
[46] Wolniak S.M., Hepler P.K., Jackson W.T., Detection of membrane-calcium distribution during mitosis in *Haemanthus* endosperm with chlortetracycline, J. Cell Biol. 87 (1980) 23–32.
[47] Hepler P.K., Callaham D.A., Free calcium increases during anaphase in stamen hair cells of *Tradescantia*, J. Cell Biol. 105 (1987) 2137–2143.
[48] Pitts K.R., Yoon Y., Krueger E.W., McNiven M.A., The dynamin-like protein DLP1 is essential for normal distribution and morphology of the endoplasmic reticulum and mitochondria in mammalian cells, Mol. Biol. Cell 10 (1999) 4403–4417.
[49] Takei K., Mundigl O., Daniell L., DeCamilli P., The synaptic vesicle cycle: a single vesicle budding step involving clathrin and dynamin, J. Cell Biol. 133 (1996) 1237–1250.